

ORIGINAL RESEARCH ARTICLE

Physicochemical Modulation of Sulfadoxine Binding to Bovine Serum Albumin: Spectroscopic and Docking Insights

Fatima I. Aliyu¹ and Kabiru. A. Musa¹ ¹Department of Biochemistry, Faculty of Basic Medical Sciences, Bayero University, Kano, Nigeria

ABSTRACT

The interaction between Sulfadoxine (SD), an antimalarial drug, and bovine serum albumin (BSA) was analyzed under varying physicochemical conditions, such as temperature (303 K, 308 K, and 313 K), pH (6.9 and 7.4), and ionic strength (0.15 and 0.2 μ M) using fluorescence, UV-Vis, FTIR spectroscopy, and molecular docking. This was done to understand the drug-protein binding mechanism and its stability during systemic transport. Fluorescence emission spectra showed gradual quenching of BSA by SD, with Stern-Volmer constants decreasing with temperature, as expected for a static quenching mechanism, and the formation of an SD-BSA complex. Thermodynamic parameters ($\Delta S = +33.90 \text{ J mol}^{-1} \text{ K}^{-1}$ and $\Delta H = -28.78 \text{ kJ mol}^{-1}$) indicated that hydrogen bonding and van der Waals forces were the stabilizing interactions, rendering moderate affinity binding (binding constant $K_a = 2.10, 2.97, \text{ and } 3.10 \times 10^4 \text{ M}^{-1}$) for all three temperatures. UV-Vis confirmed the presence of a ground-state complex, and FTIR showed changes in amide I and II bands, indicating a conformational change in the BSA. The sulfadoxine binding site was predicted using site marker displacement reactions and corroborated by molecular docking, corresponding to Sudlow's site II. These results indicated that SD-BSA interactions were regulated by pH, ionic strength, and temperature, thereby establishing a mechanistic perspective on drug distribution and efficacy under physiological or pathological conditions. The study could assist in a better understanding of the pharmacokinetics of SD in preventive malaria treatment.

ARTICLE HISTORY

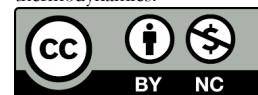
Received November 07, 2025

Accepted March 20, 2026

Published March 25, 2026

KEYWORDS

Sulfadoxine, Bovine Serum Albumin, Ligand-protein interaction, Fluorescence spectroscopy, Molecular docking, Physicochemical parameters, Binding thermodynamics.



© The Author(s). This is an Open Access article distributed under the terms of the Creative Commons Attribution 4.0 License [creativecommons.org](https://creativecommons.org/licenses/by/4.0/)

INTRODUCTION

Malaria is a major health issue facing the world, especially in sub-Saharan Africa, where the disease keeps recording high morbidity and mortality (WHO, 2023). Although chemotherapeutic methods have evolved, anti-folate drugs like Sulfadoxine (SD), which are often used as intermittent preventive therapy for pregnant women and as first-line therapy in most endemic areas, continue to play a significant role in treatment (Nikiema *et al.*, 2022). The emergence of drug-resistant strains of *Plasmodium falciparum* poses a serious threat to the effectiveness of existing antimalarial treatments, despite notable advances in malaria treatment (Siddiqui *et al.*, 2021). The typical antimalarial drugs include Pyrimethamine and Sulfadoxine, which together form Sulfadoxine-Pyrimethamine (SP) therapy, a standard treatment for uncomplicated malaria. Sulfadoxine (Figure 1) is an agent that inhibits dihydropteroate synthase, thereby affecting folate production in *Plasmodium falciparum* (De-Kock *et al.*, 2017).

Bovine serum albumin (BSA) is frequently used as a model for Human Serum Albumin (HSA) in in vitro analysis due to its structural and functional similarities. Each of the

three structurally similar domains (I, II, and III) that make up BSA has two subdomains (A and B). Its two tryptophan residues, Trp-134 and Trp-212, are located in sub-domains IB and IIA, respectively, and exhibit strong sensitivity to their immediate surroundings, which aids in the incorporation of fluorescent properties into BSA. Drug binding to BSA might therefore result in protein denaturation or conformational changes, altering the emission spectra (Bagalkoti *et al.*, 2019).

Drugs' interactions with BSA can provide important insights into their pharmacokinetics in the human body, including binding affinities, modes of transport, and overall bioavailability (Tayyab & Feroz, 2021). Drug binding to serum proteins is known to lower the concentration of free drug available for therapeutic action, which may affect treatment effectiveness and the emergence of resistance (Celestin & Musteata, 2021). Therefore, to maximize treatment options and counter the growing threat of drug resistance, a thorough understanding of the interactions between antimalarial medications and serum proteins under various

Correspondence: Kabiru. A. Musa. Department of Biochemistry, Faculty of Basic Medical Sciences, Bayero University, Kano, Nigeria. ✉ kamusa.bch@buk.edu.ng

How to cite: Aliyu, F. I. & Musa, K. A. (2026). Physicochemical Modulation of Sulfadoxine Binding to Bovine Serum Albumin: Spectroscopic and Docking Insights. *UMYU Scientifica*, 5(1), 200 – 211. <https://doi.org/10.56919/usci.2651.017>

physiological conditions is crucial (Siqueira-Neto *et al.*, 2023).

The binding of several drugs to BSA has been investigated in the past, with an emphasis on factors known to affect drug-protein interactions, such as temperature, pH, and ionic strength (Žamojć *et al.*, 2022). Modifications to these factors may change a drug's binding affinity and, consequently, its pharmacological efficacy. Nevertheless, limited studies have explored how such physicochemical variations influence the interaction between Sulfadoxine and serum albumin (Na-Bangchang & Karbwang, 2019). In this study, controlled *in vitro* conditions were provided separately to evaluate the influence of temperature, pH, and ionic strength on SD binding to Bovine Serum Albumin (BSA). This method provides essential thermodynamic, spectroscopic, and computational information on the stability and driving forces of binding interactions. The present study provides insight into the effects of pH, temperature, and ionic strength, which, to the best of our knowledge, have not been reported previously for SD-BSA interactions.

It is hypothesized that variations in physicochemical conditions significantly alter the binding affinity and stability of SD-BSA interactions, offering valuable insights into drug efficacy and guiding future antimalarial drug design strategies.

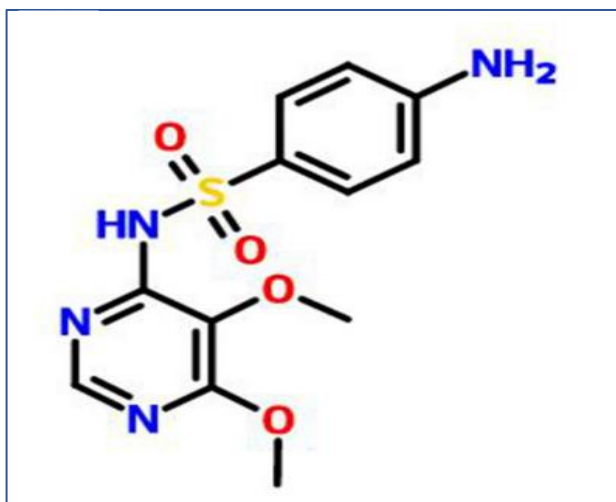


Figure 1: Chemical structure of Sulfadoxine

MATERIALS AND METHODS

Materials

Fatty acid-free bovine serum albumin (BSA) with a molecular weight of 66,500 Da, Pharmaceutical-grade Sulfadoxine (SD), and site marker ligands such as Warfarin (WFN) and ibuprofen (IF) were acquired from Haddis International Limited (Kaduna, Nigeria). Other chemicals used in this experiment, such as disodium hydrogen orthophosphate dihydrate, sodium dihydrogen orthophosphate dihydrate, and sodium chloride, were of analytical grade, and distilled water was obtained from Loba Chemie Pvt Limited (Kano, Nigeria).

Sample preparation

A stock solution of the protein was prepared by dissolving the lyophilized BSA powder in 60 mM phosphate buffer (pH 7.4) at a concentration of 20 μ M. The stock solution of 50 μ M for Sulfadoxine and site marker ligands (WFN and IF) was prepared by first dissolving measured amounts of pharmaceutical-grade Sulfadoxine powder in 10 mL of dimethyl sulfoxide (DMSO). They were further diluted to the desired volume with phosphate buffer (pH 7.4) to create a working solution suitable for the experiments (Musa *et al.*, 2021). Phosphate buffer solutions (PB) of varying pH values (6.9 and 7.4) were prepared by mixing monobasic sodium phosphate (NaH₂PO₄) and dibasic sodium phosphate (Na₂HPO₄) to simulate different conditions, allowing us to understand drug-protein interaction in different environments (Žamojć *et al.*, 2022). Additionally, the ionic strength of the buffer was varied by adding NaCl at concentrations of (μ = 0.15 and 0.2) Five sets of experiments was conducted with varying SD and BSA molar ratios (1:1, 2:1, 3:1, 4:1, 5:1, 6:1, 7:1, 8:1, 9:1, and 10:1), to study concentration-dependent binding effects (Musa *et al.*, 2020a). The concentrations were 5-50 μ M for SD and 5 μ M for BSA.

Fluorescence spectroscopy studies

Fluorescence emission spectra of BSA were recorded for each condition, both in the absence and in the presence of increasing concentrations of SD (5-50 μ M with a 5 μ M interval). Measurements were conducted using a Horiba FluoroMax-4 Spectrofluorometer equipped with a 1 cm path-length quartz cuvette. Emission spectra were recorded in the range of 300-450 nm, with an excitation wavelength set to 280 nm to selectively excite the tryptophan residues in BSA (Musa *et al.*, 2020b). To investigate how temperature affected the binding interactions, BSA solutions (5 μ M) were prepared in buffer with variable ionic strength (0.15 μ M) and pH 7.4, adjusted using NaCl. The temperature was controlled using a thermostatic water bath and set to 303 K, 308 K, and 313 K.

Sulfadoxine solution was added incrementally to the BSA sample, and changes in fluorescence intensity and peak position (λ_{max}) were monitored. Additionally, fluorescence spectra of free SD at equivalent concentrations were obtained to correct for the inner-filter effect. The data were used to calculate binding constants and determine quenching mechanisms (static or dynamic). This analysis provided detailed insights into how environmental conditions influence drug-protein interactions at the molecular level.

Fluorescence quenching data analysis

The fluorescence data were corrected for the inner filter effect using the following equation (Larsson *et al.*, 2007):

$$F_{cor} = F_{obs} 10^{(A_{ex} - A_{em})/2} \quad (1)$$

Where F_{cor} and F_{obs} refer to the corrected and the observed fluorescence intensity, respectively; A_{ex} and A_{em} denote differences in the protein absorbance at

excitation and emission wavelengths (within the range of 300–450 nm), respectively, upon SD addition. The fluorescence quenching data were analyzed using the Stern-Volmer equation:

$$F_0/F = 1 + K_{sv} [Q] \quad (2)$$

Where F_0 and F stand for fluorescence intensity values without and with SD, respectively; $[Q]$ refers to the concentration of the quencher (SD); K_{sv} is the Stern-Volmer constant. The quencher concentration $[Q]$ was varied between 5 and 50 μM , and the Stern-Volmer constant (K_{sv}) will be calculated from the slope of the F/F_0 versus $[Q]$ plot [16].

The double logarithmic equation was used to determine the binding constant (K_a) and the number of binding sites (n):

$$\text{Log} (F_0 - F/F) = \text{log} K_a + n \text{log}[Q] \quad (3)$$

A plot of $\text{log} (F_0 - F/F)$ versus $[Q]$ yields a straight line where the slope gives n , and the intercept provides K_a .

The van't Hoff plot was used to calculate thermodynamic parameters, such as the change in enthalpy (ΔH) and the change in entropy (ΔS), for the interaction between Sulfadoxine (SD) and bovine serum albumin (BSA) using the following formula:

$$\ln K_a = - (\Delta H/RT) + (\Delta S/R) \quad (4)$$

In this case, the association constant was represented by (K_a), the gas constant ($8.314 \text{ J} \cdot \text{mol}^{-1} \cdot \text{K}^{-1}$) by (R), and the absolute temperature by (T). The following relationship was used to get the values of the Gibbs free energy change (ΔG) at 303 K, 308 K, and 313 K:

$$\Delta G = \Delta H - T\Delta S \quad (5)$$

This analysis will allow for the determination of the thermodynamic forces driving the binding interactions under different temperature conditions (Musa *et al.*, 2020a).

UV-Vis spectroscopy studies

The ultraviolet (UV) absorption spectra of BSA solutions (5 μM) were recorded on a UV-Vis spectrophotometer (Perkin-Elmer UV/VIS Lambda 365) using a 1 cm path-length quartz cuvette. These tests were conducted in the 200–400 nm wavelength range. To examine how temperature, pH, and ionic strength affect binding interactions, BSA solutions (5 μM) were prepared in buffer solutions with variable ionic strengths (0.15 and 0.2 μM) and pH values (6.9 and 7.4), adjusted with NaCl. A temperature-controlled water bath was used to set the temperature to 303 K, 308 K, and 313 K (Zamojć *et al.*, 2022). UV-Vis spectra of BSA were acquired for each condition, both with and without increasing SD doses (5–50 μM with 5 μM intervals). Additionally, UV absorption spectra of free SD solutions were also acquired in the same wavelength range using the same concentrations.

FTIR spectroscopy studies

An Agilent Technologies FTIR spectrometer was used for these measurements, with spectral data recorded over 4000–400 cm^{-1} at a resolution of 4 cm^{-1} . To assess the effects of temperature, pH, and ionic strength on drug-protein interactions, BSA solutions (5 μM) were prepared in buffer solutions with variable ionic strengths (0.15 and 0.2 μM) and pH values (6.9 and 7.4), adjusted using NaCl. Temperature conditions will be controlled using a thermally jacketed sample holder and set to 303 K, 308 K, and 313 K. FT-IR spectra of BSA were recorded for each condition, both with and without SD, at two fixed molar ratios (6:1 and 12:1).

Drug solutions were added incrementally to the BSA samples, and spectra were collected after each addition to monitor changes in the amide I and amide II bands, which are sensitive to protein secondary structure. Additionally, spectra of free SD were obtained under equivalent conditions to serve as references (De-Meutter & Goormaghtigh, 2021; Mizukami *et al.*, 2022).

Site marker competitive displacement measurements

Different site markers were used to identify the presence of the SD binding sites on BSA: Ibuprofen (IF) for Site II, and warfarin (WFN) for Site I. For these analyses, a concentration of 5 μM BSA was utilized. BSA and site marker complexes were produced in a 1:1 molar ratio and incubated for 30 minutes at 303 K. In the concentration range of 5–50 μM (with an interval set for optimal data resolution), separate titrations of these samples (without and with site markers) were carried out using SD. With an excitation wavelength of 295 nm, the fluorescence spectra for SD-BSA interactions were scanned from 310 to 400 nm. For WFN, the excitation wavelength of 335 nm and the emission wavelength range of 360–480 nm were chosen (Musa *et al.*, 2020a).

Molecular docking studies

The AutoDock Vina program, interfaced with AutoDock Tools, was used for molecular docking and visualization of binding interactions. The crystal structure of BSA (PDB ID: 3V03) was retrieved from the Brookhaven Protein Data Bank (<http://www.rcsb.org/pdb>). The structure was designed to undergo preprocessing, such as adding hydrogen and charges. The BSA structure was prepared before docking by energy minimization using the Tripos force field with a distance-dependent dielectric function, and partial atomic charges were calculated using the AMBER7F9902 method in UCSF Chimera. Water molecules were removed to improve the model's accuracy in simulating drug interactions.

Sulfadoxine (SD) was drawn using ACD/ChemSketch Freeware, and its geometry was optimized to prepare the ligands using Avogadro 1.2.0 with the MMFF94s force field for energy minimization. The structures are then preprocessed, including the removal of water molecules and the addition of hydrogen atoms and Kollman charges, before docking. The grid boxes for the binding pocket were set to 70 × 70 × 70 grid points with a spacing of

0.375 Å. The resulting docking complexes were visualized in Discovery Studio Visualizer to analyze

hydrogen bonding and hydrophobic interactions (Musa *et al.*, 2021).

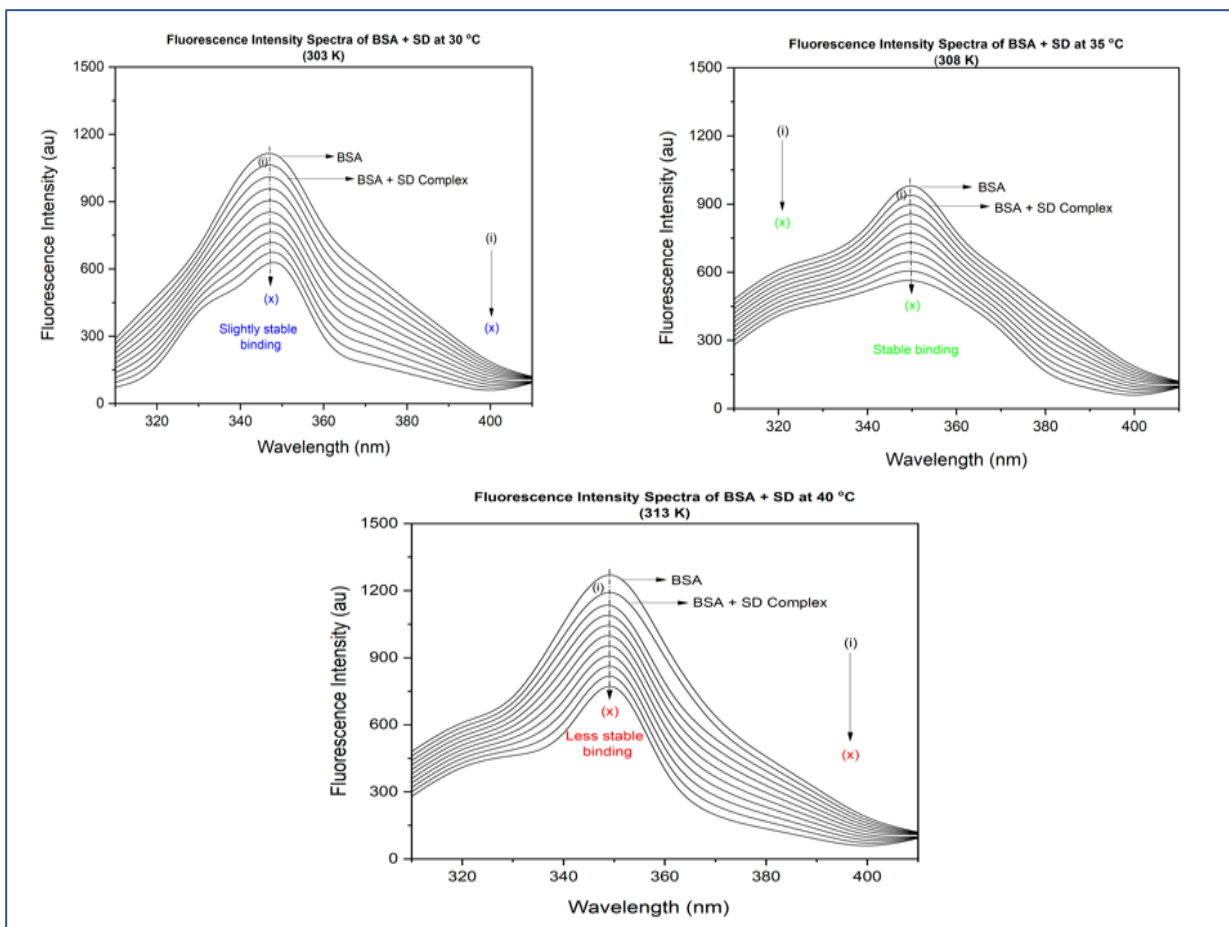


Figure 2. Fluorescence emission spectra of BSA (5 μM) in the presence of increasing concentrations of SD (5-50 μM). Measurements recorded at pH = 7.4, λ_{ex} = 296 nm, λ_{em} = 348 nm, T = 303 K, 308 K, and 313 K.

Table 1. Binding interactions and thermodynamic parameters of the SD–BSA system at various temperatures in PB 7.4.

T (K)	K _{sv} × 10 ⁴ (M ⁻¹)	K _a × 10 ⁴ (M ⁻¹)	n	ΔS (J mol ⁻¹ K ⁻¹)	ΔH (kJ mol ⁻¹)	ΔG (kJ mol ⁻¹)
303	3.27 ± 0.12	3.10 ± 0.09	1.02	—	—	-20.15
308	2.73 ± 0.07	2.97 ± 0.06	1.00	33.90	-28.78	-20.69
313	2.12 ± 0.10	2.01 ± 0.11	0.98	—	—	-20.98

Table 2. FTIR band assignments and interpretation for sulfadoxine under various conditions

C	Drug	W (cm ⁻¹)	Band Assignment	Interpretation
pH 6.9	SD	~ 1662	Amide I upshift	Increased polarity of the binding site under slightly acidic pH
IS 0.2	SD	~ 1540	Amide II	Decrease in H-bonding, weaker drug-protein complex
303 K	SD	~ 1650	Amide I slight shift	Moderate hydrogen bonding interactions
308 K	SD	~ 1656	Amide I	Stable binding environment, native-like structure retained
313 K	SD	~ 1643	Amide I significant shift	Enhanced thermal denaturation

KEY: C: Conditions; W: Wavenumber; H-bonding: Hydrogen bonding

Table 3. Predicted hydrogen bond interactions between SD and amino acid residues of BSA at the binding site.

Ligand	Binding site	Protein atom	SD atom	Distance (Å)
SD	Sudlow's site II	Asp323:OD1	H	2.02
		Arg208:NH1	H	1.88

Electrostatic potential surface mapping

Electrostatic potential maps were generated to evaluate the influence of environmental conditions such as pH levels (6.9 and 7.4) and ionic strengths (0.15 and 0.2 μM) and temperatures (303 K, 308 K, and 313 K) on the

protein's electrostatic surface. The docked complex files (complex.pdb) were converted to PQR format using the PDB2PQR server, with the appropriate protonation state for each simulated condition. Electrostatic potential calculations were performed using the Adaptive Poisson-Boltzmann Solver (APBS) via its web interface. The

resulting DX files were loaded into UCSF Chimera, and the electrostatic surface was mapped using a color gradient representing positive and negative potential regions.

Visualizations were saved in high-resolution image format for interpretation and reporting (Zhou & Pang, 2018; Rathi *et al.*, 2020).

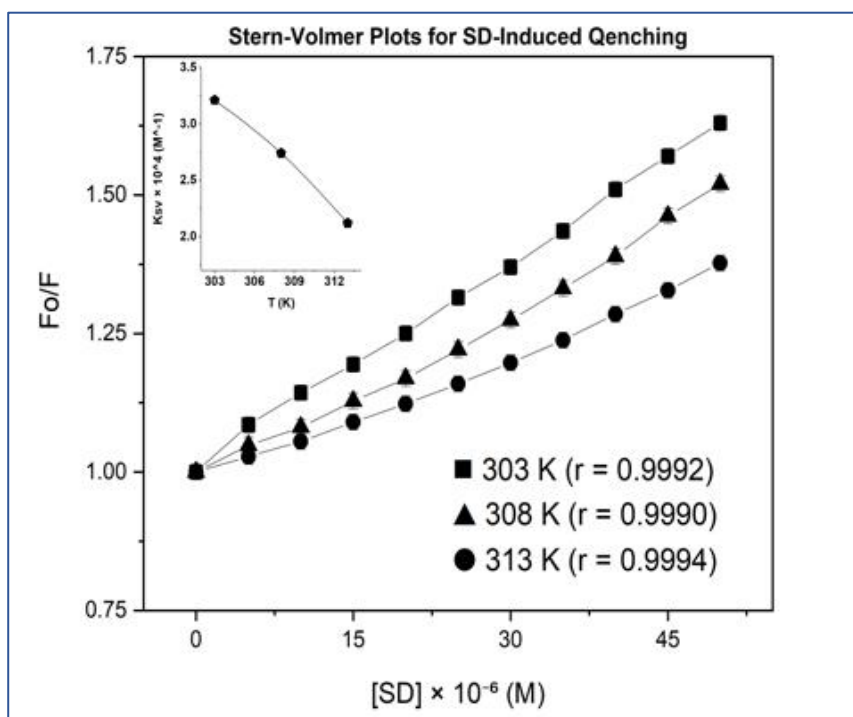


Figure 3. Stern-Volmer curves for quenching of SD with BSA at 303 K, 308 K, and 313 K. Inset shows the temperature-induced decrease in the Ksv value.

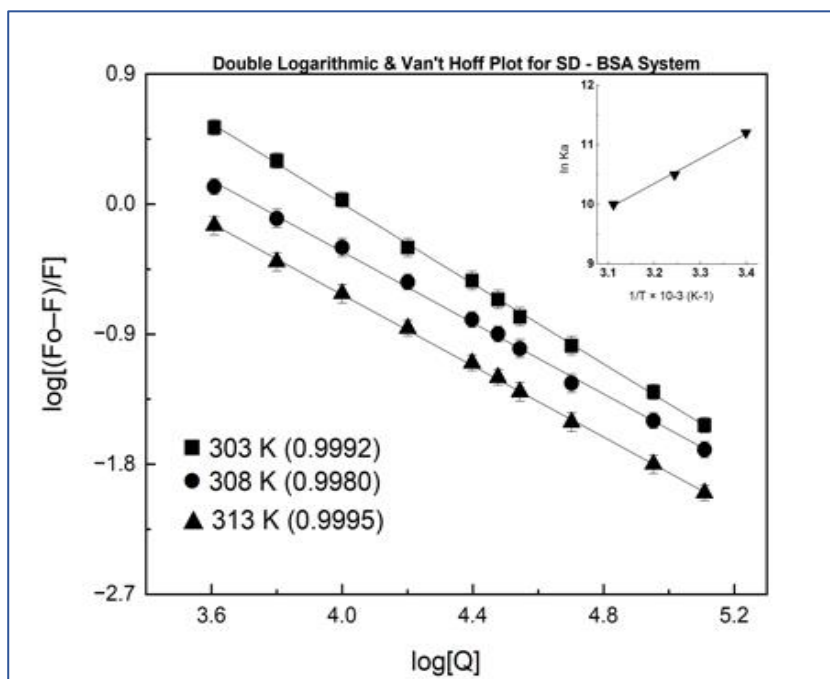


Figure 4. Double-logarithmic plots for the SD – BSA System at 303, 308, and 313 K. Inset depicts a van't Hoff plot for determining thermodynamic parameters.

Statistical Analysis

At least three trials were performed for each experiment to ensure accuracy and repeatability. To show the variability in the measurements, the results were provided as the mean ± standard deviation (SD). OriginPro 2022 (OriginLab Corp., Northampton, MA) was used for statistical analysis, including curve charting and result interpretation.

RESULTS AND DISCUSSION

Characterization of the quenching behavior of sulfadoxine on bovine serum albumin

Fluorescence spectra of BSA (5 uM) were taken after adding Sulfadoxine (5-50 uM) in three tests with incremental addition of Sulfadoxine at three temperatures (303 K, 308 K, and 313K) in the presence of phosphate

buffer (295 nm). Sulfadoxine had no intrinsic fluorescence at this wavelength, and any change in the emission spectra was guaranteed to occur only as a result of drug-induced quenching of BSA fluorescence (Figure 2). A gradual

increase in Sulfadoxine concentration led to a concentration-dependent increase in the intensity of BSA fluorescence, but did not significantly shift the emission maxima (~342 nm).

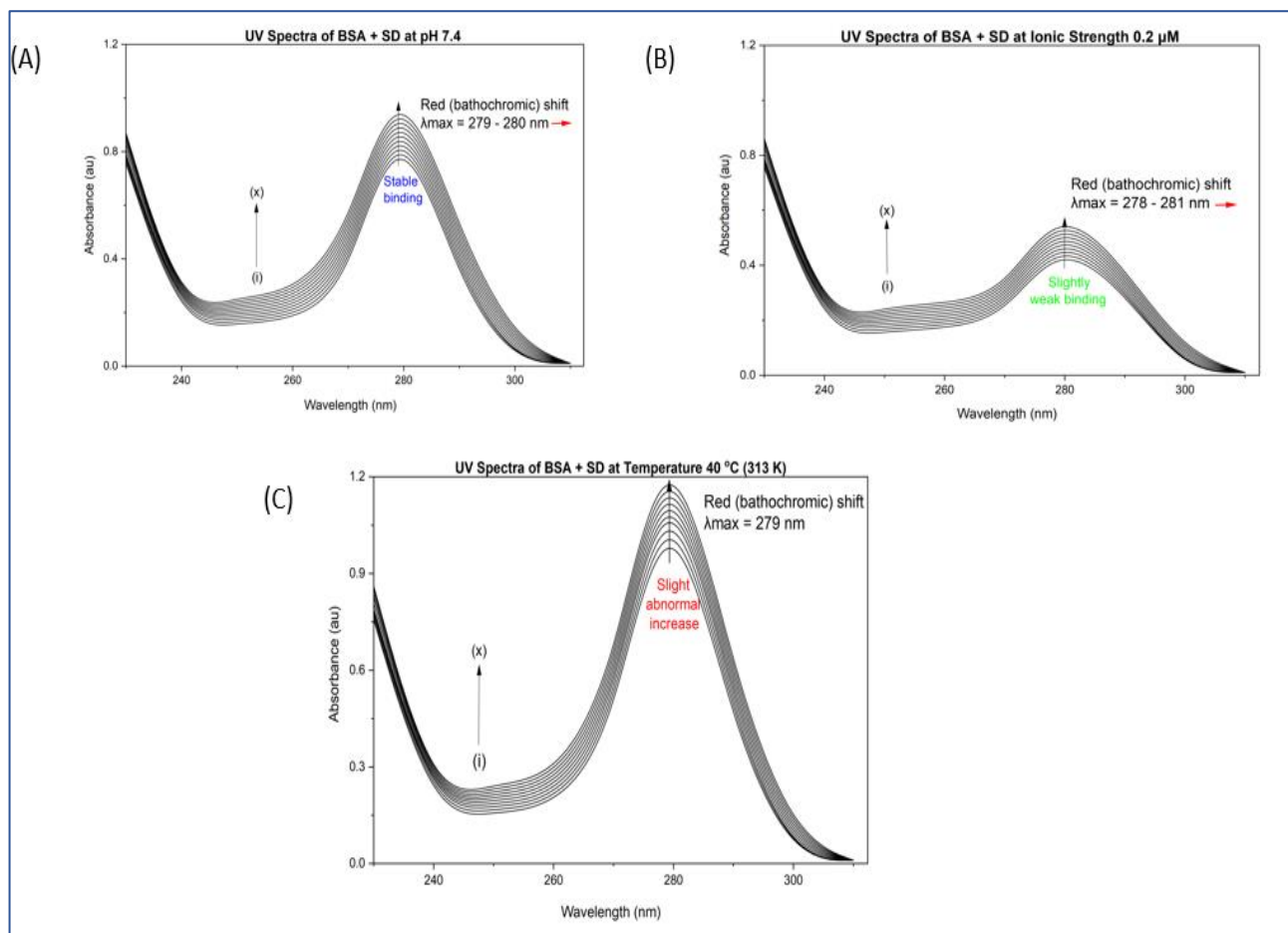


Figure 5. UV-Vis absorption Spectra of SD – BSA Complex at pH 7.4. Spectra recorded at varying temperatures and ionic strength conditions showing absorbance changes at 279 nm.

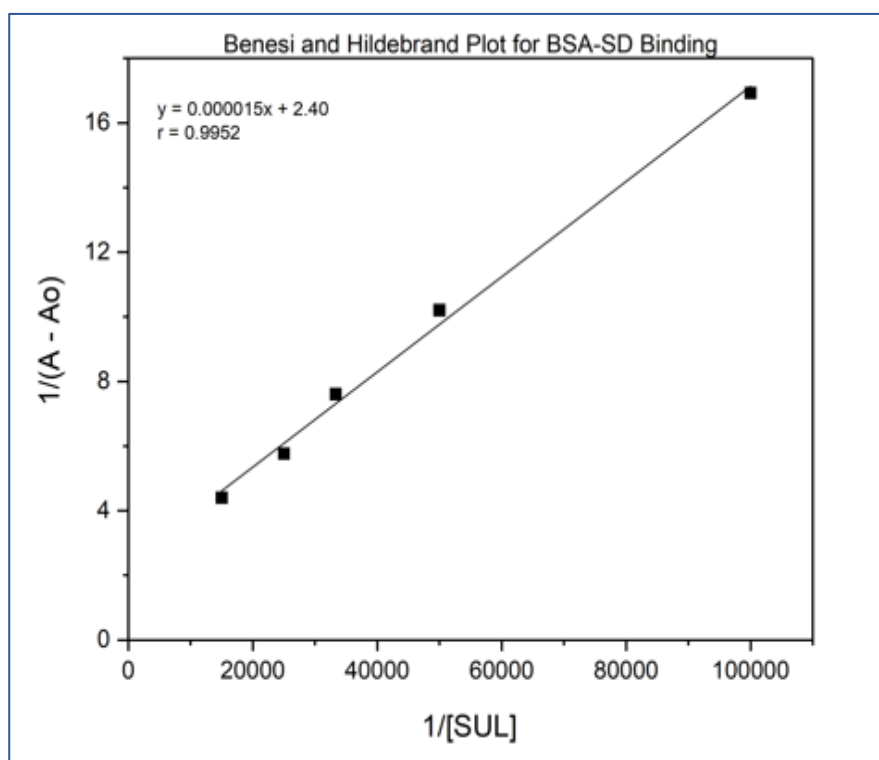


Figure 6. Benesi-Hildebrand plots for the interaction of SD with BSA at pH 7.4.

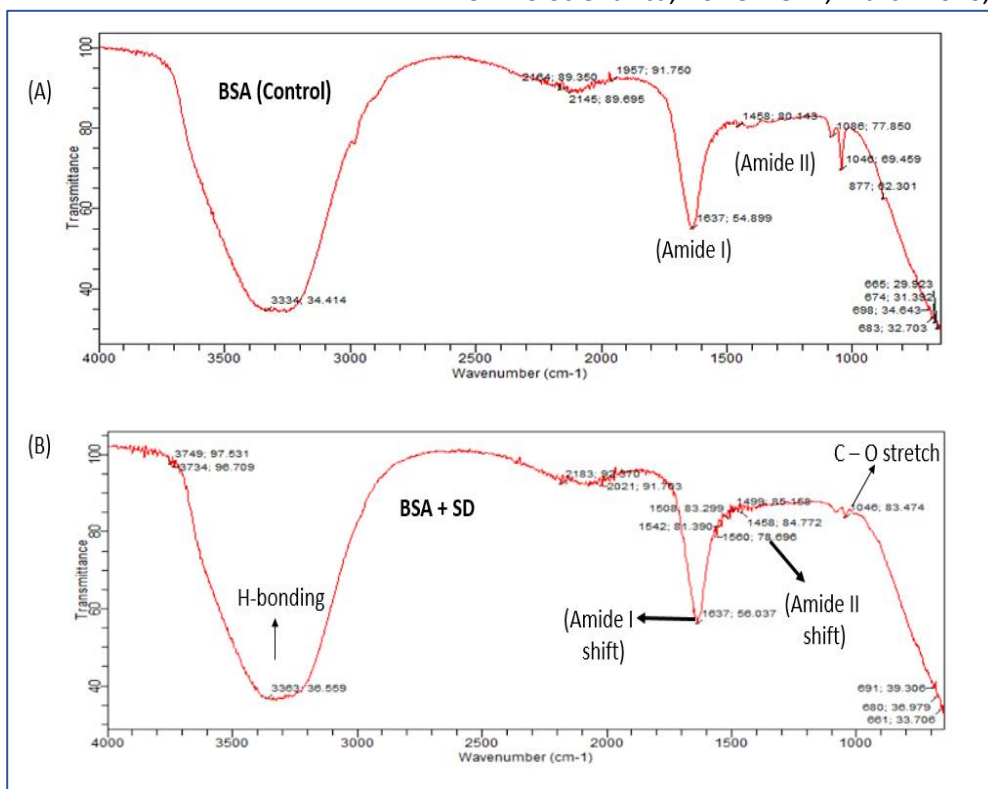


Figure 7. FTIR spectra of BSA and SD-BSA complex (12:1).

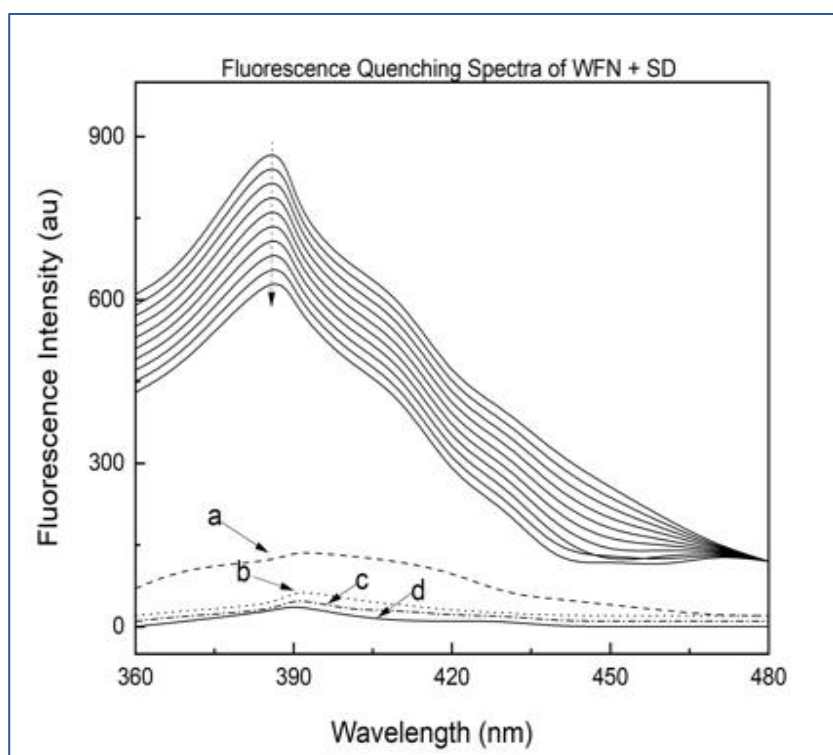


Figure 8. Fluorescence spectra of WFN-BSA complex (1:1) in the presence of increasing SD concentrations (5-50 μM). Spectra recorded in phosphate buffer (pH 7.4).

At the three temperatures (303 K, 308 K, and 313 K), Stern-Volmer plots of Sulfadoxine were straight (Figure 3). The Stern-Volmer quenching constant (K_{sv}), as shown in Table 1, decreased with increasing temperature, as expected for a static quenching mechanism ($2.12 \times 10^4 M^{-1}$ and $3.27 \times 10^4 M^{-1}$). The number of binding locations (n) and the binding constant (K_a) were obtained from the double logarithmic plots (Figure 4). The calculated n

values were about 1.0, implying the existence of a single binding site. The K_a values varied between $2.01 \times 10^4 M^{-1}$ and $3.10 \times 10^4 M^{-1}$ (Table 1), which means that the affinity between SD and BSA is moderate.

Fluorescence quenching analysis confirmed interaction between SD and BSA via static quenching, indicating the existence of a stable ground-state complex. This mechanism was supported by the linearity of the Stern-

Volmer plots observed and by the decrease in the value of K_{sv} as temperature increased. The binding constant K_a ($2.01-3.10 \times 10^4 M^{-1}$) was calculated and is in the range of

values typical of drug protein systems, indicating moderate levels of affinity that allow an effective delivery of a drug and release at the target site.

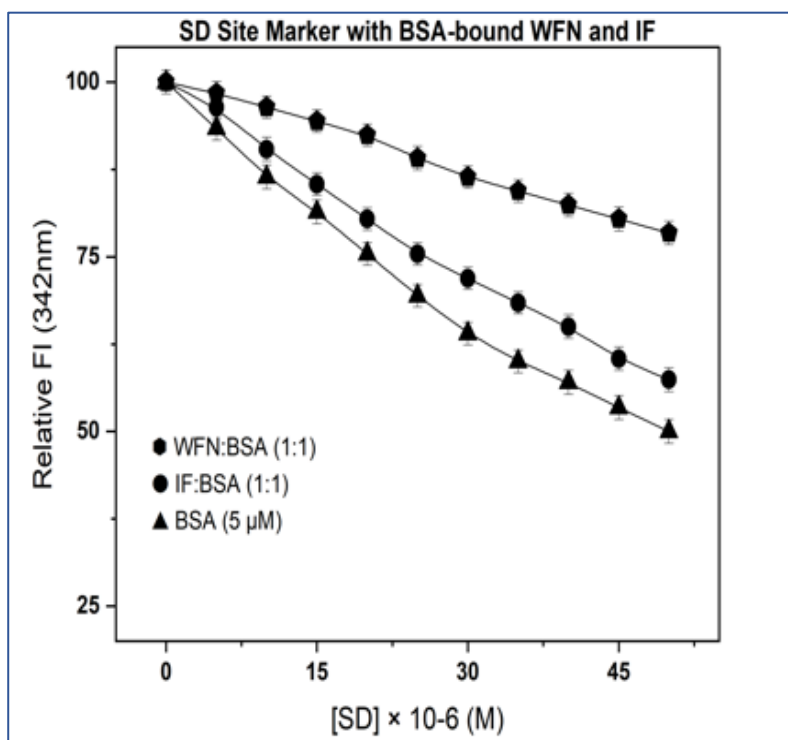


Figure 9. Displacement of WFN and IF with rising from their BSA-bound forms upon addition of Sulfadoxine (5-50 μM). Fluorescence intensity monitored at 342 nm in phosphate buffer (pH 7.4).



Figure 10. Docked pose of SD within BSA showing binding orientation at Sudlow's site IIA. The ligand is shown in stick representation with interacting residues highlighted.

Thermodynamics parameters

The Van't Hoff equation (Fig. 4) was used to estimate thermodynamic data and determine changes in Gibbs free energy (ΔG), enthalpy (ΔH), and entropy (ΔS). At all

temperatures, the calculated ΔG values were negative (-19.84 to -20.44 kJ/mol), indicating that the binding process is spontaneous (Table 1). The change in enthalpy ($\Delta H = -29.18$ kJ/mol) was negative, and the change in entropy ($\Delta S = 30.50$ J/mol-K) was positive.

Spontaneous and exothermic binding was observed in the thermodynamic parameters (ΔG , ΔH , ΔS), mainly through hydrophobic and hydrogen bonding. The negative ΔH is the indication of exothermic interaction, and the positive ΔS is the indication of higher randomness as a result of

the displacement of water as a result of the hydrophobic pockets occupied by the complex on its formation. These results correlate with other reports of protein-ligand binding (Bagalkoti *et al.*, 2019; Musa *et al.*, 2020a; Žamojć *et al.*, 2022).

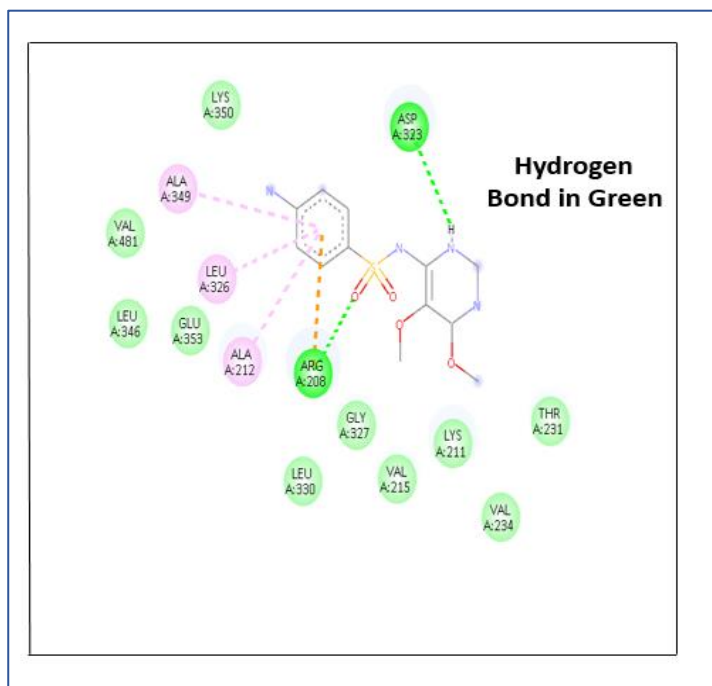


Figure 11. 2D interaction diagram of the SD-BSA complex generated using Discovery Studio.

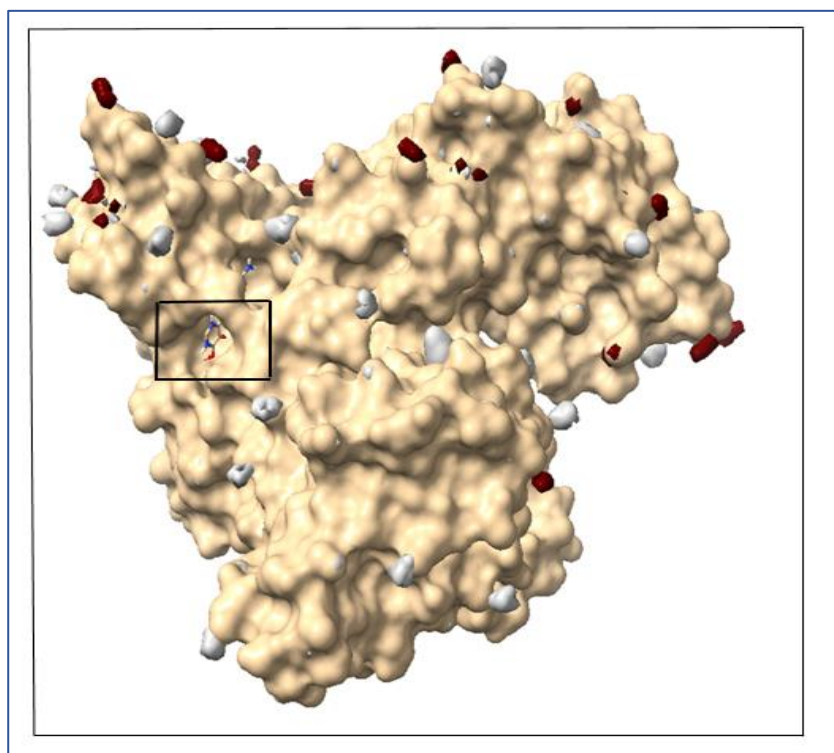


Figure 12. Electrostatic potential surface map of the SDBSA complex at pH 7.4, 310 K, and ionic strength 0.15 μM . The ligand is displayed in stick representation against a surface colored by electrostatic potential.

UV-Visible absorption analysis

At various pH (6.9 and 7.4), temperatures (303 K, 308 K, 313 K), and ionic strengths (0.15 M, 0.20 M), the UV-Vis absorption spectra of BSA differed upon collision with an alternate solution of varying SD concentration. BSA was

left alone, showing a characteristic absorption peak at 279 nm and a maximum absorbance of about 0.80 at a near-optimum temperature of 308 K, pH 7.4, and 0.15 ionic strength. When SD was added, the absorbance intensity changed with concentration. When the ionic strength was increased (0.2 M), the absorbance was less, and this was

an indication that binding was less, as a result of electrostatic shielding. The same situation was observed at pH 6.9. Conversely, there was a rapid increase in

absorbance at 313 K, which could be attributed to conformational relaxation and the uncovering of binding sites (Figure 5).

Table 4. Summary of environmental effects on ligand binding affinity and electrostatic characteristics.

C	L	BE (kcal/mol)	Electrostatic Observation	Affinity Trend
pH 6.9	SD	-6.9	Optimal potential environment	Optimal
pH 7.4	SD	-6.9	Optimal potential environment	Strong
IS 0.15	SD	-6.8	Good electrostatic contrast	Strong
IS 0.2	SD	-6.7	Reduced charge contrast	Mild decrease
303 K	SD	-6.9	Stable surface	Strong
308 K	SD	-6.8	High complementary potential across the binding pocket	Strong
313 K	SD	-6.6	Partial screening, but interactions maintained	Moderate-weak

KEY: C: Conditions; L: Ligands; BE: Binding Energy;

The plot made by Benesi-Hildebrand with these data was linear, indicating 1:1 stoichiometry and suggesting the possibility of stable complex formation. The closest linear equation to the pH 7.4 condition was $y = 0.000015x + 2.40$; $r = 0.9952$, indicating a high linear correlation and a medium binding affinity (Figure 6).

The UV-Vis spectral analysis was consistent with the fluorescence results and demonstrated quenching of the statistics and the 1:1 stoichiometry of the complexes. Increased absorbance with temperature indicates conformational flexibility in the protein, which prefers interaction at high temperature, whereas higher ionic strength reduced the binding, probably because excess ions electrostatically shielded the binding.

Fourier transform infrared (FTIR) spectroscopy.

The FTIR spectra of BSA and SD-BSA complexes were taken in diverse conditions of temperatures (303-313 K), pH (6.9 and 7.4), ionic strength (0.15-0.20 M) and molar ratios (6:1 and 12:1). The amide I (around 1650 cm^{-1}) and amide II (around 1540 cm^{-1}) bands were observed to change significantly which indicated changes in the way the BSA was in its conformation in case of SD binding (Table 2).

The shift of the amide I band to 1637 cm^{-1} (aqueous) and the decrease in transmittance were the indicators of the partial binding of an α -helical structure by a ligand through the creation of structural changes. The other alterations were observed in the OH/NH stretching region (3425 cm^{-1}) and the C=O stretching region (1994-2008 cm^{-1}), which provide additional evidence of hydrogen-bond interactions (Figure 7). These studies were also confirmed by FTIR analysis, which revealed changes in the amide I and II bands, which represented the opening of the α -helix and hydrogen bonding. The spectral shifts substantiated changes in conformational arrangements upon ligand binding, with dose-dependent intensity changes depending on the SD concentrations.

Site probe study

Fluorescence displacement assays with Warfarin (Site I marker) and Ibuprofen (Site II marker) revealed that SD selectively interacts with Sudlow's site II. Fluorescence displacement assays indicated that with increasing amounts of SD in the mixture, there was a significant

reduction in Ibuprofen fluorescence (~380-390 nm), indicating a competitive interaction at Site II (Figure 8). The less effective quenching of the Warfarin-BSA system indicated a decreasing affinity for Site II (Figure 9).

Molecular docking analysis

AutoDock Vina Molecular docking studies of SD with BSA indicated 12 conformational clusters. The highest population cluster of 38 out of 100 conformations yielded an average binding energy of -6.5 kcal/mol, and the best pose had a binding energy of -5.3 kcal/mol. Some of the major interacting residues in the 5 A of SD were Ala349, Asp323, Ala212, Asp323, and Leu326, which comprised a hydrophobic pocket that is stabilized by hydrogen bonds between Asp323 and Arg208 (Table 3; Figure 10-11).

The experimental results were structurally validated by molecular docking in which SD was localized to a hydrophobic cavity caused by the arrangement of Ala349, Asp323, Ala212, Asp323, and Leu326. A binding energy of -6.5 kcal/mol was observed, indicating a stable and desirable interaction, which is similar to the experimental K_a values.

3.7 Electrostatic potential surface mapping

The electrostatic mapping method provides visual data on how the environment affects ligand binding stability. The effects of environmental conditions on the electrostatic potential map of the SD-BSA complex and the subsequent effect on binding affinity are summarized in Table 4. The electrostatic analysis also favors the finding that binding of ligand is most optimized under near physiological conditions (pH 7.4, 308 K, 0.15 M IS), at which the potential surface is most complementary to charge distribution on the ligand (Figure 12). This observation suggests that sulfadoxine binding may remain stable in physiological environments with slight pH variations. Such stability is particularly relevant in disease conditions or physiological states that may influence blood pH.

Taken together, these spectroscopic and computational findings support the overall idea that SD stably and selectively interacts with BSA through hydrophobic and hydrogen-bond interactions that depend on temperature, pH, and ionic concentration variations, and therefore

imply the significance of the physiological environment in drug-protein interactions.

This research highlights the applicability of serum albumin associations in adjusting the pharmacokinetics of Sulfadoxine, with implications for optimizing dosing regimens, especially under conditions of altered physiology, such as fever, pregnancy, or inflammation. Subsequent investigations employing *in vivo* experiments should be undertaken to reaffirm these *in vitro* findings and also examine how dynamic the plasma conditions were on drug bioavailability and efficacy.

CONCLUSIONS

This study examined the interaction of Sulfadoxine (SD) with Bovine Serum Albumin (BSA) under different physicochemical conditions, i.e., temperature, pH, and ionic strength. The drug demonstrated static quenching via fluorescence quenching spectroscopy, indicating the formation of stable ground-state complexes between the drug and BSA. The Stern-Volmer graphs showed that the binding strength decreases with increasing temperature, confirming that the quenching phenomenon is very much static and suggesting complex destabilization at higher thermal energy. Thermodynamic modeling showed that the reactions are spontaneous. Thermodynamic parameters ($\Delta S = +33.90 \text{ J mol}^{-1} \text{ K}^{-1}$ and $\Delta H = -28.78 \text{ kJ mol}^{-1}$) indicate that hydrogen bonding and van der Waals forces were the stabilizing interactions, rendering moderate affinity binding (the binding constant $K_a = 2.97 \times 10^4 \text{ M}^{-1}$). The change in entropy ΔS of the two drugs indicates different forces of binding; The ΔS of Sulfadoxine is entropy-disfavored; thus, hydrogen bond or van der Waals forces.

BSA-drug complex formation was supported by complementary UV-Vis spectroscopic analysis, which showed a hyperchromic and bathochromic shift. The structural perturbations in BSA, especially in the amide I and II regions, were also supported by the FTIR spectra, which confirmed that drug binding caused conformational perturbations. Site mark displacement experiments carried out with warfarin (Site I) and ibuprofen (Site II) also showed site-specific affinity: SD was consistent with docking predictions, indicating its preferential binding within Sudlow's site II.

The study provided us with knowledge of drug-protein interactions under practical biological conditions. It contributed to the science of drug delivery and to the profiling of serum protein interactions, and it provided a basis for pharmacokinetic simulation, providing value to formulation scientists, drug designers, and therapeutic modelers. Further studies should aim to assess the interaction between Sulfadoxine and Human Serum Albumin across a wider range of physiological and pathophysiological conditions, including variations in glucose levels, oxidative stress, and disease states. Incorporating *in vivo* pharmacokinetic studies or simulations could help establish real-time distribution, half-life, and clearance rates for these antimalarial drugs under different physiological conditions.

ETHICS STATEMENT

There were no human and animal subjects in this research. All the laboratory work was conducted in line with institutional and international ethical standards for laboratory research.

CONFLICT OF INTEREST

Authors declare no competing financial or personal interests regarding this study.

FUNDING

This research received no specific grant from any funding agency in the public or commercial sectors.

ACKNOWLEDGEMENTS

The authors are very thankful to the Department of Biochemistry, Bayero University, Kano, Nigeria, for allowing the use of laboratory facilities and technical support during the research.

DATA AVAILABILITY

The datasets generated during this study are available upon request. Additional spectra, raw data, and computational files are included in the supplementary material.

REFERENCES

- Bagalkoti, J. T., Joshi, S. D., & Nandibewoor, S. T. (2019). Spectral and molecular modelling studies of sulfadoxine interaction with bovine serum albumin. *Journal of Photochemistry and Photobiology A: Chemistry*, 382, 111871. [[Crossref](#)]
- Celestin, M. N., & Musteata, F. M. (2021). Impact of changes in free concentrations and drug-protein binding on drug dosing regimens in special populations and disease states. *Journal of Pharmaceutical Sciences*, 110(10), 3331-3344. [[Crossref](#)]
- De Kock, M., Tarning, J., Workman, L., Nyunt, M. M., Adam, I., Barnes, K. I., & Denti, P. (2017). Pharmacokinetics of sulfadoxine and pyrimethamine for intermittent preventive treatment of malaria during pregnancy and after delivery. *CPT: Pharmacometrics & Systems Pharmacology*, 6(7), 430-438. [[Crossref](#)]
- De Meutter, J., & Goormaghtigh, E. (2021). Evaluation of protein secondary structure from FTIR spectra improved after partial deuteration. *European Biophysics Journal*, 50(3-4), 613-628. [[Crossref](#)]
- Koundal, S., Pathania, A., Kour, H. D., Pathania, A. R., Kaur, J., Juneja, B., Sharma, G. C., Bhowmik, A., & Santhosh, A. J. (2025). Molecular interaction study of L-ornithine with bovine serum albumin using spectroscopic and molecular docking methods. *Scientific Reports*, 15(1), 1-16. [[Crossref](#)]
- Larsson, T., Wedborg, M., & Turner, D. (2007). Correction of inner-filter effect in fluorescence excitation-emission matrix spectrometry using Raman scatter. *Analytica Chimica Acta*, 583(2),

- 357-363. [\[Crossref\]](#)
- Lyndem, S., Hazarika, U., Athul, P., Bhatta, A., Prakash, V., Jha, A. N., & Singha Roy, A. (2023). A comprehensive in vitro exploration into the interaction mechanism of coumarin derivatives with bovine hemoglobin: Spectroscopic and computational methods. *Journal of Photochemistry and Photobiology A: Chemistry*, 436, 114425. [\[Crossref\]](#)
- Mizukami, T., Bedford, J. T., Liao, S. H., Greene, L. H., & Roder, H. (2022). Effects of ionic strength on the folding and stability of SAMP1, a ubiquitin-like halophilic protein. *Biophysical Journal*, 121(4), 552-564. [\[Crossref\]](#)
- Musa, K. A., Ning, T., Mohamad, S. B., & Tayyab, S. (2020a). Intermolecular recognition between pyrimethamine, an antimalarial drug and human serum albumin: Spectroscopic and docking study. *Journal of Molecular Liquids*, 311, 113270. [\[Crossref\]](#)
- Musa, K. A., Ridzwan, N. F. W., Mohamad, S. B., & Tayyab, S. (2020b). Combination mode of antimalarial drug mefloquine and human serum albumin: Insights from spectroscopic and docking approaches. *Biopolymers*, 111(2), e23337. [\[Crossref\]](#)
- Musa, K. A., Ridzwan, N. F. W., Mohamad, S. B., & Tayyab, S. (2021). Exploring the combination characteristics of lumefantrine, an antimalarial drug and human serum albumin through spectroscopic and molecular docking studies. *Journal of Biomolecular Structure and Dynamics*, 39(2), 691-702. [\[Crossref\]](#)
- Na-Bangchang, K., & Karbwang, J. (2019). Pharmacology of antimalarial drugs. In *Encyclopedia of malaria* (1-82). [\[Crossref\]](#)
- Nikiema, S., Soulama, I., Sombié, S., Tchouatieu, A. M., Sermé, S. S., Henry, N. B., Ouedraogo, N., Ouaré, N., Ily, R., Ouédraogo, O., Zongo, D., Djigma, F. W., Tiono, A. B., Sirima, S. B., & Simporté, J. (2022). Seasonal malaria chemoprevention implementation: Effect on malaria incidence and immunity in a context of expansion of Plasmodium falciparum resistant genotypes. *Infection and Drug Resistance*, 15, 4517-4527. [\[Crossref\]](#)
- Rathi, P. C., Ludlow, R. F., & Verdonk, M. L. (2020). Practical high-quality electrostatic potential surfaces for drug discovery using a graph-convolutional deep neural network. *Journal of Medicinal Chemistry*, 63(16), 8778-8790. [\[Crossref\]](#)
- Siddiqui, F. A., Liang, X., & Cui, L. (2021). Plasmodium falciparum resistance to ACTs: Emergence, mechanisms, and outlook. *International Journal for Parasitology: Drugs and Drug Resistance*, 16, 102-118. [\[Crossref\]](#)
- Siqueira-Neto, J. L., Wicht, K. J., Chibale, K., Burrows, J. N., Fidock, D. A., & Winzeler, E. A. (2023). Antimalarial drug discovery: Progress and approaches. *Nature Reviews Drug Discovery*, 22(10), 807-826. [\[Crossref\]](#)
- Tayyab, S., & Feroz, S. R. (2021). Serum albumin: Clinical significance of drug binding and development as drug delivery vehicle. *Advances in Protein Chemistry and Structural Biology* (Vol. 123, pp. 1-30). Elsevier. [\[Crossref\]](#)
- Vaughns, C. (2007). Stern-Volmer quenching of conjugated polymers: A study of fluorophore concentration. 1-22. [\[Link\]](#)
- World Health Organization. (2023). World malaria report 2023. [\[Link\]](#)
- Żamojć, K., Wyrzykowski, D., & Chmurzyński, L. (2022). On the effect of pH, temperature, and surfactant structure on bovine serum albumin-cationic/anionic/nonionic surfactants interactions. *International Journal of Molecular Sciences*, 23(1), 41. [\[Crossref\]](#)
- Zhou, H. X., & Pang, X. (2018). Electrostatic interactions in protein structure, folding, binding, and condensation. *Chemical Reviews*, 118(4), 1691-1741. [\[Crossref\]](#)